

Prediction of Seasonal Forest Fire Severity in Canada from Large-Scale Climate Patterns

AMIR SHABBAR AND WALTER SKINNER

Science and Technology Branch, Environment Canada, Toronto, Ontario, Canada

MIKE D. FLANNIGAN

Canadian Forest Service, Great Lakes Forestry Centre, Sault Ste. Marie, Ontario, and Department of Renewable Resources, University of Alberta, Edmonton, Alberta, Canada

(Manuscript received 28 April 2010, in final form 19 November 2010)

ABSTRACT

An empirical scheme for predicting the meteorological conditions that lead to summer forest fire severity for Canada using the multivariate singular value decomposition (SVD) has been developed for the 1953–2007 period. The levels and sources of predictive skill have been estimated using a cross-validation design. The predictor fields are global sea surface temperatures (SST) and Palmer drought severity index. Two consecutive 3-month predictor periods are used to detect evolving conditions in the predictor fields. Correlation, mean absolute error, and percent correct verification statistics are used to assess forecast model performance. Nationally averaged skills are shown to be statistically significant, which suggests that they are suitable for application to forest fire prediction and for management purposes. These forecasts average a 0.33 correlation skill across Canada and greater than 0.6 in the forested regions from the Yukon, through northern Prairie Provinces, northern Ontario, and central Quebec into Newfoundland. SVD forecasts generally outperform persistence forecasts. The importance of the leading two SVD modes to Canadian summer forest fire severity, accounting for approximately 95% of the squared covariance, is emphasized. The first mode relates strongly to interdecadal trend in global SST. Between 1953 and 2007 the western tropical Pacific, the Indian, and the North Atlantic Oceans have tended to warm while the northeastern Pacific and the extreme Southern Hemisphere oceans have shown a cooling trend. During the same period, summer forest fire exhibited increased severity across the large boreal forest region of Canada. The SVD diagnostics also indicate that the El Niño–Southern Oscillation and the Pacific decadal oscillation play a significant role in Canadian fire severity. Warm episodes (El Niño) tend to be associated with severe fire conditions over the Yukon, parts of the northern Prairie Provinces, and central Quebec. The linearity of the SVD manifests opposite response during the cold (La Niña) events.

1. Introduction

Wildland fire is a dominant disturbance regime in Canadian forests, particularly in the boreal forest region where fire is a process critical to the very existence of primary boreal species such as pine, spruce, and aspen and is responsible for shaping landscape diversity and influencing energy flows and biogeochemical cycling (Stocks et al. 2002). Stocks et al. (1996) examined the spatial distribution of large fires in Canada during the 1980s when an average of almost 10 000 fires burned

over 2.8 million ha annually. They found that by far the greatest area burned occurred in the boreal region of west-central Canada. This was attributed to a combination of factors including fire-prone ecosystems, extreme fire weather, lightning activity, and varying levels of protection in this region. The number of wildland fires, as well as the total area burned (TAB) by wildland fire in Canada, has steadily increased since 1960, with the reported area burned in some regions of the country tripling from 1980 to the present (Stocks et al. 2002). In Canada the majority of the fire activity occurs from late April through August in the south and from June to August in the north, with most of the area burned occurring from June to August during which time higher temperatures and thunderstorms with lightning strikes occur most

Corresponding author address: Amir Shabbar, 4905 Dufferin St., Toronto ON M3H 5T4, Canada.
E-mail: amir.shabbar@ec.gc.ca

frequently. Nearly 50% of the area burned in Canada is the result of fires that are not acted on because of their remote location, low values at risk, and efforts to accommodate the natural role of fire in these ecosystems.

The release of carbon dioxide and other greenhouse gases from biomass burning contributes to global warming (Stocks et al. 2002; Amiro et al. 2009). It is therefore important to identify climatic factors, such as slow-varying boundary conditions, that may contribute to an extended forest fire season in Canada. Gillett et al. (2004) demonstrated that human-induced climatic change has significantly affected the TAB by forest fires in Canada by first using output from a coupled climate model to show that greenhouse gas and sulfate aerosol emissions have made a detectable contribution to summer-season warming in regions of Canada where the area burned by forest fires has increased and then applying a statistical model to simulate temperature changes.

The daily severity rating (DSR) index is part of the Canadian forest fire weather index (FWI) system (van Wagner 1987) and is a numerical rating that reflects the amount of effort required to suppress a fire. The DSR is derived from daily measurements of precipitation, air temperature, humidity, and wind. The DSR, when averaged over a season, is termed the seasonal severity rating (SSR) index. The SSR can be used as an objective measure of the fire weather/climate from season to season and from region to region. On a routine basis, Natural Resources Canada (2009) uses SSR as a management tool for historical analysis as well as for operational long-range forecasts (see online at http://cwfis.cfs.nrcan.gc.ca/en_CA/background/summary/). Balshi et al. (2008) recently employed the monthly severity rating (MSR), or the monthly component of the SSR, as input when modeling future fire in the North American boreal forest. Skinner et al. (2006) examined coupled modes of variability between the SSR index and the previous winter global sea surface temperatures (SSTs) using singular value decomposition (SVD) analysis. They found the leading three SVD modes accounted for approximately 90% of the squared covariance of Canadian summer forest fire severity. The first mode is related to the global long-term trend and shows significant positive correlation in the forested regions of northwestern, western, and central Canada. The second mode is related to the multidecadal variation of Atlantic Ocean SST, identified as Atlantic multidecadal oscillation (AMO; Enfield et al. 2001), and shows statistically significant negative correlation extending from the western Northwest Territories and the Canadian Prairie Provinces across northern Ontario and Quebec. The third mode is related to Pacific Ocean processes and the interrelationship between El Niño–Southern Oscillation (ENSO) and the Pacific decadal oscillation (PDO; Mantua et al. 1997)

and shows statistically significant positive correlation in western Canada and negative correlation in the lower Great Lakes region of southern Ontario and southern Quebec.

In Canada, the physical and economic impacts of extended dry conditions are most evident during the warm season. A statistically robust relationship between seasonal Canadian temperature and precipitation, key factors in the formation of conditions leading to fire severity, and the ENSO cycle has already been established (Shabbar and Khandekar 1996; Shabbar et al. 1997). Bonsal and Lawford (1999) have related variations in tropical Pacific SSTs to regional Canadian prairie dry spells. The establishment and persistence of extended dry spells most likely favor forest conflagration elsewhere in Canada. Skinner et al. (2002) have shown the close geographical association across Canada between anomalous ridging in the midtroposphere at 500-hPa geopotential heights and TAB by wildland fire in the summer season.

This is the first study that has focused on summer-season forest fire severity in the context of moisture conditions in Canada and ocean–atmosphere forcing mechanisms during several preceding seasons. Westerling et al. (2002) employed a statistical forecast method to predict area burned in western U.S. wildfires a season in advance from the Palmer drought severity index (PDSI). In the Canadian context, Meyn et al. (2010) report a strong association between anomalous drought conditions as inferred from PDSI immediately prior to the fire season and area burned at most of the higher-elevation sites in British Columbia and the Yukon.

Evidence for the lagged relationship between summer climate variability in Canada and preceding winter tropical SSTs exists in observational data. For example, Shabbar and Barnston (1996) identified the ENSO cycle, which achieves its highest magnitude during the boreal winter, as the main source of variability in producing skillful forecasts of Canadian temperatures and precipitation from winter into early summer. As well, Rajagopalan et al. (2000) found a coupled pattern between summer drought over the continental United States and winter SST variability during the twentieth century. The influences of large-scale global ocean teleconnection patterns in determining summer extreme moisture conditions over Canada have also been documented by Shabbar and Skinner (2004). It was found that dry conditions in Canada coincide with warmer-than-normal SSTs in the equatorial eastern Pacific, along the North American west coast, and in the North Atlantic. Conversely, wet summer conditions in Canada coincide with colder-than-normal SSTs in the previous winter, in the central equatorial Pacific, and along the North American west coast, indicative of the cold phase of ENSO. It is important to understand better the variability

of biomass burning with respect to evolving climatic conditions on global, hemispheric, and continental scales.

For these reasons, summer-season forest fire data are analyzed by the multivariate spatial technique of SVD to assess the utility of antecedent winter and spring global SST anomalies and Canadian drought index for the purpose of seasonal fire-severity prediction. Winter climate conditions can directly affect soil and forest fuel moisture capacity in the ensuing months. The purpose of this study is twofold. First, the strength and nature of the lagged relationship between global SST and the PDSI (predictors) and the SSR (predictand) fields are assessed. The diagnostics that accompany SVD provide some insight into the physical processes of the teleconnections. Second, an algorithm for the skillful guidance for seasonal forecasting of SSR for Canada is devised. The remainder of the paper is organized as follows: the datasets are described in section 2, the SVD diagnostic and prediction methods are described in section 3, and the diagnostic and prediction results are outlined in section 4. The paper closes with a summary and discussion in section 5.

2. Data

a. Canadian forest fire SSR

One measure of forest fire severity is TAB by wildland fire. The data distribution is poor, with a low number of points and irregular spatial distribution. The TAB is a function of many factors (some not related to weather) whereas the SSR is a function solely of weather variables. Therefore, a closer relationship between climate (SST and PDSI) patterns and SSR can be expected. As a result, a second measure of forest fire severity was employed, the DSR index. In Canada, the DSR is an extension of the FWI system. See the appendix for a more detailed description of the Canadian FWI system.

The severity of a fire season is a function of a number of factors: fuel, including the weather (temperature, precipitation, humidity, wind, synoptic patterns, and others); ignition agents (human and lightning); fuel characteristics (fuel type, structure, and moisture of fine surface fuels and deeper organic fuels); and human activities (land use and management). However, the weather is the key factor in determining the severity of the fire season (Flannigan and Wotton 2001). The SSR is the DSR averaged monthly and/or seasonally. These two measures of forest fire severity are fully described and compared in Skinner et al. (2006).

DSR has been calculated from Environment Canada synoptic weather data from 1953 to 2007 and interpolated to a grid using a thin-plate cubic-spline method (Flannigan and Wotton 1989). This method was found to be the best-suited interpolation technique applied to a multivariate

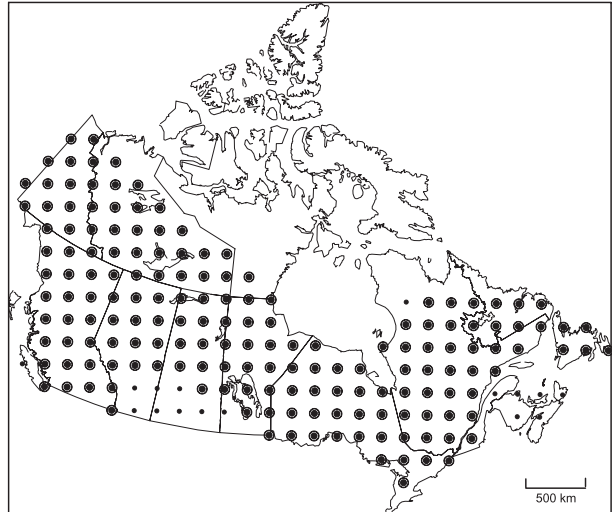


FIG. 1. SSR grid at approximately 200-km spacing. Grid points used in this analysis (larger dots with circles) are based on percent total annual area burned being greater than 1% of the national total. Regions covered by the small dots were not analyzed because they cover areas of less than 1% of the national total.

index of this type. A minimum of 12 weather stations were used for each gridpoint interpolation, though more were used if available. The weather stations closest to the grid point were chosen first using an expanding search radius until at least 12 active stations were found. The interpolated data were then averaged monthly and seasonally. Figure 1 shows the data grid across Canada on an approximate 200-km spacing used in this study. The 169 grid points designated with large dots were used in this study. The SSR has a much larger number of points and a more comprehensive gridded spatial distribution than does the TAB statistic. Regions in Fig. 1 covered by the small dots were not used because the percent annual area burned is less than 1.0% of the national total (Stocks et al. 2002). Both Canada and the United States have developed this and other forest fire weather indices to monitor conditions for fire potential across the forested regions of North America using both manned and remote networks. The SSR can also be useful for historical analysis and in long-range forecasts for use as a management tool. The time series of summer (June–August) SSR from 1953 to 2007 (55 years) is shown in Fig. 2 for Canada. For comparison purposes, the TAB time series for the 1959–99 period is also shown in Fig. 2. The correlation between TAB and SSR is 0.42 for the 41 overlapping years (significant at 99%). High SSR (TAB) values indicate greater fire severity and vice versa. In general, SSR in western Canada had a few high years in the late 1950s and early 1960s (1955, 1958, and 1961), it was low through the 1970s and into the 1980s, and it has shown a considerable increase over the past two decades.

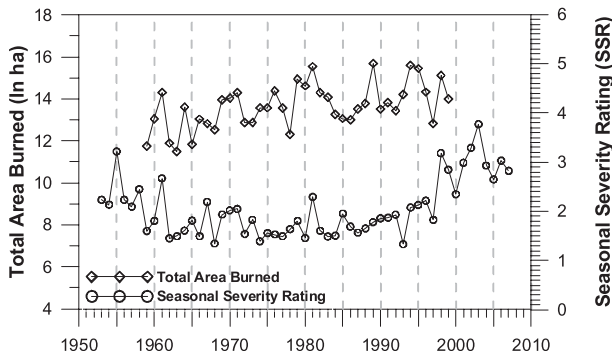


FIG. 2. Summer (June–August) SSR from 1953 to 2007 and TAB from 1959 to 1999 for Canada. The correlation between TAB and SSR is $r = 0.42$ for 1959–99.

b. Climatic data

Global SST on a 2° latitude–longitude grid for the 1953–2007 period came from the Extended Reconstruction Sea Surface Temperatures, version 3, (ERSSTv3) dataset (Smith et al. 2008). They calculated the anomalies relative to the 1960–90 base period over 10 988 latitude–longitude locations. The reconstruction of the data involves a rigorous quality-control procedure and a statistical analysis methodology that is an improvement over their previous version ERSSTv2 (Smith and Reynolds 2005). Bias-adjusted satellite SSTs are added to ERSSTv2, thus providing a better resolution as well as resolving more variance in the southern oceans. The satellite-based ice analyses are bias adjusted to improve the high-latitude SST analysis. The anomaly reconstruction is performed separately for the low- and high-frequency components, and the sum of these components constitutes the total SST anomaly. To extract dominant modes of SST variability, empirical orthogonal function (EOF) analysis of the cross-covariance matrix is carried out on the winter averages.

Large forest fires in Canada are related to variations in global SST. A number of numerical modeling studies have established linkages between secular warming trend in SSTs and anomalous midlatitude atmospheric ridging (Hoerling and Kumar 2003). By subscribing warmer-than-normal SSTs in the western Pacific and Indian Oceans in the Geophysical Fluid Dynamic Laboratory climate model, Lau et al. (2006) produced anomalous ridging in the midlatitudes, leading to warmer and drier conditions in the Pacific–North American sector that are conducive to large forest fires in Canada.

The PDSI has been a commonly used drought index in North America and was developed to measure intensity, duration, and spatial extent of drought. The computational procedure is described by Palmer (1965) and Alley (1984). The PDSI has become the primary tool for describing and monitoring prevailing drought. The PDSI

model allows measurement of prolonged abnormal dryness or wetness across a region and can be related directly to past weather conditions. Monthly or seasonal PDSI values reflect moisture inputs and balances not only during the current season but also over the previous several months, including winter snowfall and storage. It is thus absolutely necessary to have accurate winter precipitation (mainly snowfall) measurements for the soil moisture account. Winter PDSI reflects previous summer and autumn moisture conditions, and spring PDSI reflects both spring conditions and previous summer and autumn moisture conditions as well as overwinter storage.

A number of studies have related occurrences of forest fires to ongoing drought conditions in North America. In Canada, Meyn et al. (2010) used a drought index (PDSI) to examine trend variations in forest fire in British Columbia. A large percentage of the Canadian boreal forest is peatlands/wetlands for which a longer-term drought is required for fire to occur (Turetsky et al. 2004). Girardin and Wotton (2009) examined summer moisture, in the form of the monthly drought code (part of the FWI system) across Canada for the 1901–2002 period. Xiao and Zhuang (2007) found a strong relationship between moisture conditions (PDSI) and forest fire activity in Canada and Alaska during 1959–99, and several studies have examined drought-induced fire occurrences in the western United States (e.g., Collins et al. 2006; Keeton et al. 2007; Littell et al. 2009; Kitzberger et al. 2007), as well as in the eastern United States (Mitchener and Parker 2005).

The PDSI has been computed for approximately 100 Canadian stations from the homogenized Canadian historical air temperature and precipitation database of climatic stations, having collocated monthly mean air temperature (Vincent and Gullett 1999) and monthly total precipitation (Mekis and Hogg 1999) records extending from 1953 or earlier and updated to the end of 2007. Monthly PDSI values for 344 contiguous U.S. climate divisions obtained from the National Climatic Data Center were added to the Canadian data to provide more complete spatial coverage for analysis at the international border. All North American data were objectively interpolated at approximately 250 km^2 , and data representing grid squares north of 40°N were further analyzed. Averages were calculated for the winter and spring seasons over 271 grid locations.

3. Analysis

a. Choice of predictors

Based on previous experimentation in Canada (Shabbar and Skinner 2004) and the findings of other studies, winter-season interannual-to-decadal-time-scale global

SST anomaly patterns have accounted for the following summer predictability in moisture conditions in Canada. Thus, the built-in memory of moisture in the PDSI from the previous two seasons can be a useful indicator of summer SSR. Given the gridding of predictor fields and their usage over two consecutive prior seasons, there is a total of 22 518 $[2(10\,988 + 271)]$ predictor elements for SSR prediction over 169 grid locations.

b. SVD

The SVD method relates two fields by decomposing their covariance matrix into singular values and two sets of paired orthogonal vectors, one for each field (Bretherton et al. 1992). The covariance between the expansion coefficients of the leading pattern in each field is maximized. The singular values give the magnitude of the squared covariance fraction (SCF) as accounted for by the various singular values (Wallace et al. 1992). The square of any singular value between two fields for a given mode is indicative of the fraction of the total squared covariance accounted for by that mode. The teleconnections between the two fields are discerned by the spatial patterns of the heterogeneous correlation, which is defined here as the serial correlation between the expansion coefficients of predictor time series and gridpoint anomaly values of the predictand field.

An SVD predictor loading pattern for a given mode consists of a set of two (previous winter and spring) temporally staggered spatial patterns that are related to the mode's predictand loading pattern. This sequence of predictor patterns expresses the evolving nature of ENSO as well as the drought conditions as accounted by the PDSI. This scenario subsequently relates to the predictand pattern. In this study, the large-scale relationships between winter (December–February) and spring (March–May) patterns of global SSTs and Canadian PDSI are used to predict patterns of following-summer (June–August) fire severity in Canada. It is found that SVD accounts for trends and emphasizes ENSO and low-frequency modes such as the Pacific decadal oscillation. This technique has been used by Shabbar and Skinner (2004) and Skinner et al. (2006) to identify relationships between SST patterns and summer drought and summer forest fire severity, respectively.

c. Data preprocessing and preorthogonalization

Prior to the SVD analysis, the predictor and predictand are standardized, field weighted, and then separately preorthogonalized using standard EOF analysis. The correlation-based EOF analyses reduce the large number of original dimensions to many fewer dimensions capturing low-frequency, and presumably predictable, components. Interfield weighting is performed in the manner that prescribed relative weight of different predictors.

Fields of greater importance—for example, global SST—are usually given higher weights than other predictors. Because of the slow-varying and sustained boundary forcing of global SST, comparatively higher weights are assigned to global SST than to other predictors in statistical prediction schemes (e.g., Barnston 1994). Based on a series of forecast-skill sensitivity experiments, the SST elements are given double the weight of the PDSI elements in the study presented here. Shabbar and Barnston (1996) also showed that the dominant source of skill in the prediction of Canadian climate originates from global SST. Interfield weighting also equalizes the relative dominance of two fields when one contains fewer elements than the other. In this study, the interdecadal trend in the global oceans is shown to have a definite predictive relationship with the seasonal severity rating index in Canada. In addition, the time–space behavior of the SST field related to ENSO influences the forest fire climate in Canada (Skinner et al. 2006). The SVD diagnostics provide some insight into the statistical relationship between the predictor and predictand fields.

For the preorthogonalization of the predictors, data from the past two nonoverlapping seasons (forming a temporal sequence) enter the process together, producing an extended EOF analysis. On the basis of signal-to-noise considerations, EOF mode is truncated at five for the predictor series and six for the predictand series. The truncation preserves about 55% of the original predictor variance and about 70% of the original predictand variance.

Following the above procedure, the input cross-dataset covariance matrix for the SVD is constructed. An SVD truncation of five modes is used, allowing for full utilization of the input EOF time series. The SVD predictor loading pattern for a given mode consists of a set of two temporally staggered spatial patterns that are preferred with respect to the mode's predictand loading pattern. The sequence of predictor loading patterns (SVP) expresses a physically meaningful temporal evolution relating to the principal predictand map. The two respective associated time series (SVT), with one value per year, show the temporal behavior of SVP.

d. Verification

To avoid artificial skill in statistical forecasting models, which may stem from overfitting of random variability in a relatively short (55 years) period, a cross-validation framework (Michaelsen 1987) is adopted. In this scheme, prediction models are developed over the length of the time series with one year held in abeyance. The forecast is then verified on the withheld year. In reality, omission of a single observation in the cross-validation procedure may still introduce bias into the estimation of forecast skill. In the presence of serial correlation in climate noise,

the removal of a single observation may be replaced by the removal of blocks of observations (Shabbar and Kharin 2007). In this study, forecast skill is evaluated for both 1-year-out and 3-years-out cross-validation frameworks. In the 3-years-out scheme, forecast is verified on the middle year. The forecast target data are avoided in the development of the prediction algorithm at all stages. This includes pre-EOF steps as well as the SVD model. When performing EOF and SVD for each cross-validated model, it is possible that the SVD patterns may change as different years are left out. Another caveat is that the order of SVD modes may also change. However, since the first five modes account for most of the covariance fraction, these considerations will not significantly alter the verification statistics, as reported in section 4b. The predictor data for the withheld year are then projected onto the predictor SVP loading patterns, and predictand values are generated and verified against observed data for the withheld year. Here it is assumed that the SVD patterns are orthonormal. The climatology is redefined each time a new year (or a block of years) is held out as the forecast target. Persistence of the predictand is computed and used as a standard against which the SVD forecast is compared. To verify a persistence forecast in a cross-validation framework, the persistence forecast is formed using a different coefficient as a function of the target year, based on the autocorrelation computed from the nontarget years. Skill scores evaluated in a non-cross-validated framework were only slightly better than those calculated in the cross-validation framework.

e. Skill score

A number of skill scores are used to measure forecast model performance. A temporal correlation (CORR) between the forecasts and the observations is used as a verification measure. Although correlation is a good measurement of linear association between the forecasts and observations, it does not take forecast bias into account and is sensitive to outliers. The mean absolute error (MAE) measures the average magnitude of the forecast errors. MAE is an unambiguous measure of the average error (Willmott and Matsuura 2005). Skill score is also calculated for categorical forecasts as percent correct (PERCOR). Assuming a Gaussian distribution for SSR, the forecasts are categorized into three equiprobable classes of below normal, near normal, and above normal based on a 3×3 contingency table.

4. Results

Predictive skill results for the SSR field at the 169 grid locations are evaluated by examining average skill across Canada as well as the geographical distribution of the

seasonal skill. In addition, insight into the oceanic and surface moisture spatial patterns leading to the skillful SSR forecasts is investigated by examining the leading modes of the SVD loading patterns of the predictors and predictands.

a. Source of SSR predictability

The contribution of the predictors to the skill of the forecasts is assessed by examining the SVD loading patterns in time. The source of the skill resides in those areas of the loading patterns exhibiting high magnitude. Figure 3a shows the first SVD pattern S1(SSR) and standardized amplitude based on data for 55 summer (June–August) seasons. It is by far the most dominant mode and explains 75.8% of the total variance of Canadian SSR, and it has positive loadings over much of the forested region of Canada and opposite negative loadings only in a small area of southern British Columbia. The time series for S1(SSR) shows evidence of positive trend, particularly since the mid-1970s. It will be shown that this mode of the SSR has its origin mainly in the global-scale long-term SST trend.

Figure 3b shows the spatial pattern associated with S2(SSR). It is a secondary, but important, mode and explains 18.8% of the total variance. It identifies mainly negative loadings across Canada, with stronger negative loadings in northwestern Canada (Yukon), across the central Prairie Provinces (Alberta–Saskatchewan–Manitoba), and eastern Labrador and Newfoundland. Strong positive loadings are evident in the Mackenzie River basin and the St. Lawrence lowlands. The time series for S2(SSR) shows little evidence of long-term variability and has extreme conditions early in the record (1953 and 1955). It will be shown that this mode of the SSR has its origin mainly in Pacific Ocean processes—namely, the ENSO and PDO phenomena.

The spatial patterns, or trend at every grid point, associated with S1(SST, PDSI) are shown in Fig. 4a for winter and Fig. 4b for spring. Lower PDSI values denote drier conditions. Figure 4c shows the standardized amplitude for the predictor S1 mode. This mode identifies distinct trends in the SSTs, with strong positive loadings in the Indian Ocean and western Pacific as well as the entire North Atlantic Ocean. Negative loadings are evident in the extreme southern oceans and the north-central Pacific Ocean. A similar SST loading pattern has been reported by Smith and Reynolds (2003), who identified a trend mode in their second rotated EOF of the global SSTs, and by Skinner et al. (2006), who identified this SST pattern in their first SVD mode when examining the relationship between winter SSTs and summer forest fire severity in Canada. This mode also identifies the AMO signal, with positive loadings in the

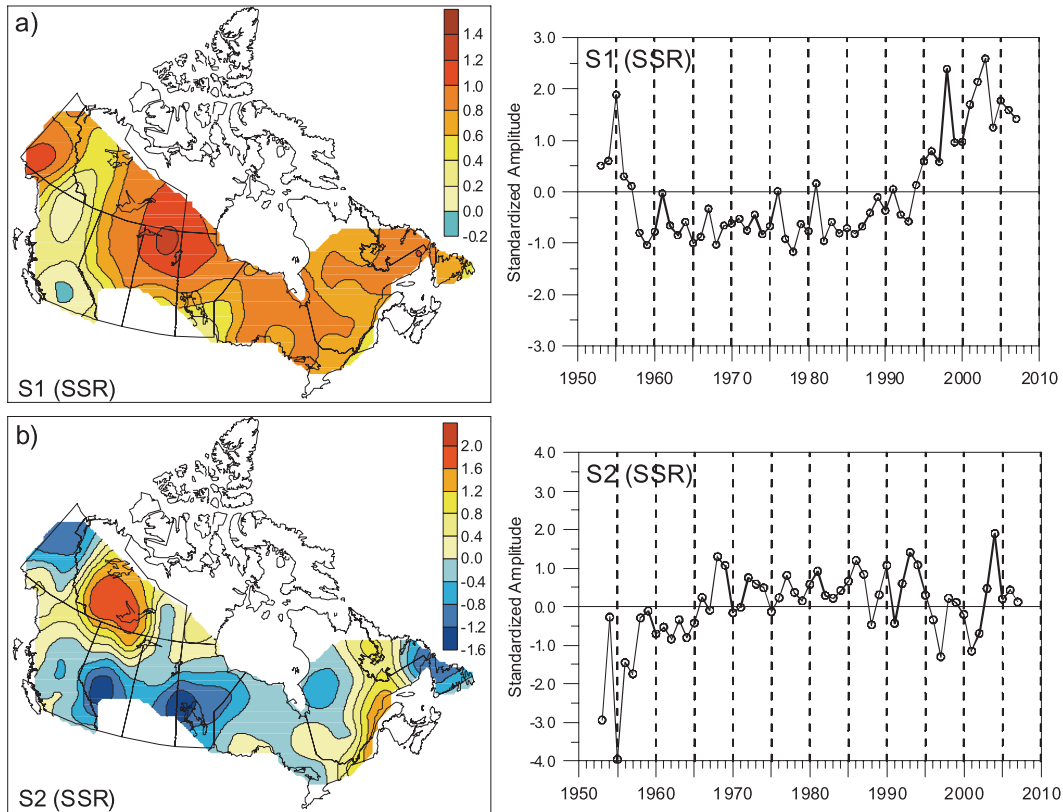


FIG. 3. (a) First SVD pattern (S1) of SSR and standardized amplitude based on data for 55 summer (June–August) seasons 1953–2007; (b) as in (a) but for the second SVD pattern (S2) of SSR and standardized amplitude.

entire North Atlantic Ocean. Variability of the Atlantic processes at varying time scales was previously identified by Shabbar and Skinner (2004). The winter and spring PDSI patterns show negative loadings (dry conditions) across most of the country with the exception of the Mackenzie River basin region of the Northwest Territories. The time series (Fig. 4c) for S1(SST, PDSI) exhibits strong positive trend since 1965.

The second SVD patterns associated with S2(SST, PDSI) are shown in Fig. 5a for winter and Fig. 5b for spring. Figure 5c shows the standardized amplitude for the S2 mode. The Fig. 5c time series also identifies extremes in ENSO years delineated by positive (El Niño) and negative (La Niña) values. The dominant SST features in this mode appear to be mixed between the tropical Pacific Ocean (ENSO) and the North Pacific Ocean (PDO). The S2 SST patterns identify strong positive loadings in the tropical and subtropical Pacific Ocean from 180° to the coast of South America (warm ENSO) and along the North American west coast, with another opposing negative center in the North Pacific (positive PDO). Previous studies have identified the coexistence of these two sources of variability. Zhang et al. (1997) found a similar mode while examining

wintertime variability in their high-pass (interannual) filtered SSTs. Pacific SST variations are evident in this mode, including the effects of ENSO in the eastern equatorial Pacific and the extratropical SST fluctuations in the central North Pacific, resembling the coupled ocean–atmosphere PDO mode. The winter and spring PDSI patterns are mixed but in general show negative loadings (dry conditions) across southwestern and central Canada and the Mackenzie River basin region of the Northwest Territories and positive loadings (wetter conditions) in the Yukon and eastern Canada. Figure 5c also shows evidence of multidecadal variability with what appears to be an increasing trend over the period of record, with a distinct positive change in the mid-1970s.

Table 1 shows the three main summary statistics of the SVD analysis for Canadian summer SSR data, preceding winter and spring global SST anomaly data, and Canadian PDSI data. These statistics provide a measure of the strength of the relationship between the two fields. The first statistic, the SCF, provides the percentage of the total squared covariance between the two fields explained by the SVD mode and is proportional to the square of its singular value. This is a measure of the relative importance of the SVD mode in the relationship

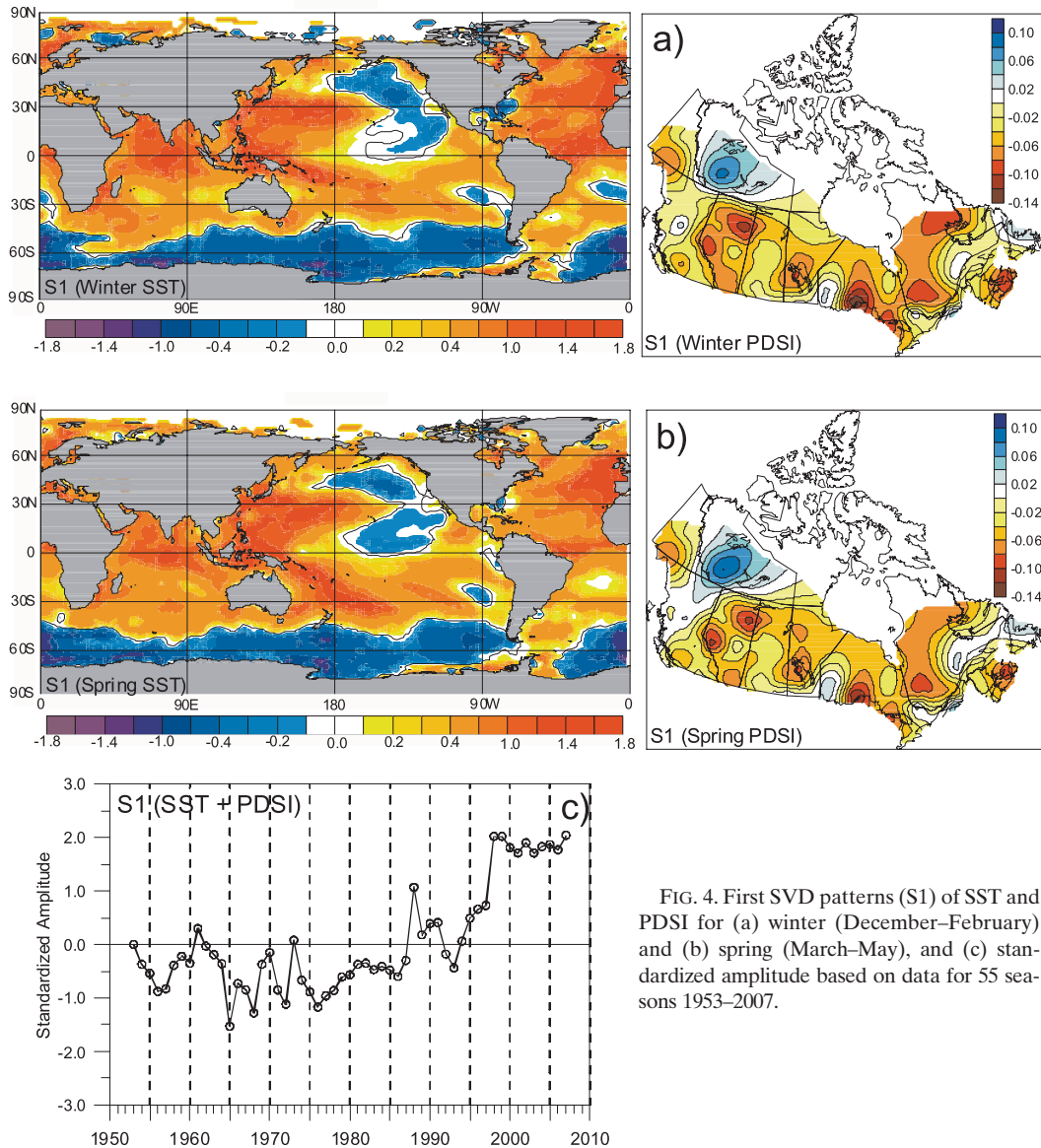


FIG. 4. First SVD patterns (S1) of SST and PDSI for (a) winter (December–February) and (b) spring (March–May), and (c) standardized amplitude based on data for 55 seasons 1953–2007.

between the two fields. It is clear from Table 1 that the squared covariance is concentrated in the first two modes (close to 95%), with the first mode being dominant (close to 76%). Thereafter, the squared covariance statistic drops off sharply, thus signifying the importance of the first two modes in determining SSR variability. The second statistic is the correlation coefficient r between the two time series that represent the temporal variations of the mode in the two fields. It is a measure of the similarity between the time variations of the patterns of the two fields, or how closely the two fields are related to each other. The relationship is strong for the first mode ($r = 0.78$), as well as the second mode ($r = 0.56$), both significant at the 5% level. The significance test was

adjusted for the autocorrelation, taking effective degrees of freedom into consideration. The third statistic, the normalized root-mean-square covariance fraction (NCF), is the ratio of the squared singular value of the mode to the greatest possible total squared covariance. It is a measure of the absolute importance of the SVD mode in the relationship between the two fields and is the most revealing statistic in the analysis. Approximately 21% of NCF is concentrated in the first two modes of the SVD expansion. The values are about equally distributed and drop off in higher modes, again emphasizing the importance of these modes in relation to higher modes. In summary, the first two modes explain a large portion of variance in individual fields, the

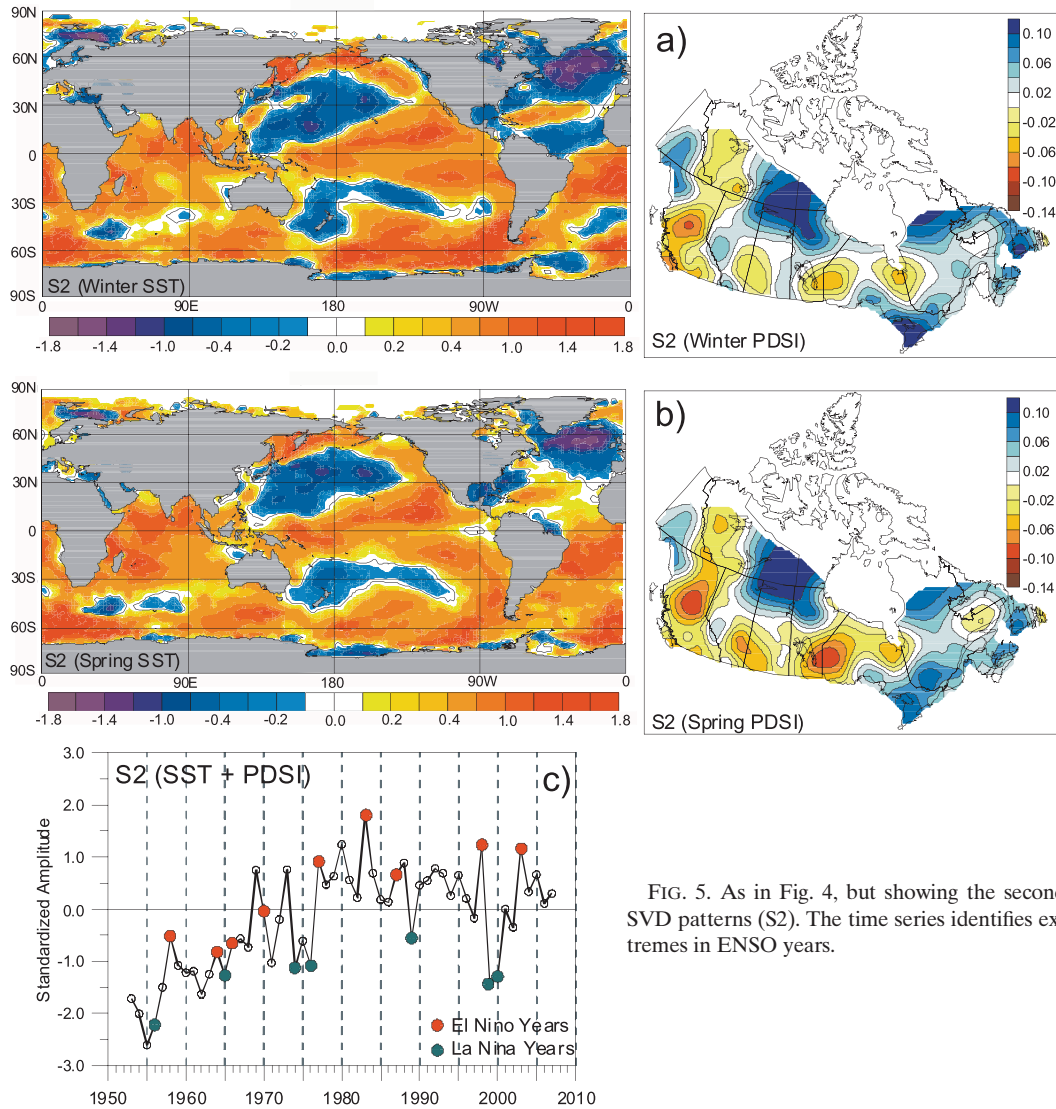


FIG. 5. As in Fig. 4, but showing the second SVD patterns (S2). The time series identifies extremes in ENSO years.

correlation between predictor and predictand time series is high, and the squared covariance fractions are large. These statistics indicate that these modes likely have some physical meaning and are not purely a statistical artifact.

Figure 6a shows the heterogeneous correlation pattern of SSR for the first mode in the direct SVD expansion using global SSTs and Canadian PDSI and Fig. 6b shows the same for the second heterogeneous correlation pattern of SSR. The heterogeneous correlation patterns show how the two fields are related to one another and how much of the amplitude of the variations is explained by the SVD mode. The heterogeneous pattern for the first SVD mode (Fig. 6a) has two prominent features: the warming of the global oceans, as indicated by the positive loadings in the Indian Ocean and western

Pacific as well as the entire North Atlantic Ocean, and the negative loadings in the north-central Pacific and low PDSI values across most of Canada (Fig. 4) are associated with high SSR across much of the forested region of Canada. Previous studies (Shabbar and Skinner 2004; Skinner et al. 2006) have also identified this link between global ocean positive anomalies and dry conditions over Canada (Fig. 3a). Positive SSR correlation (high fire severity corresponding to a warming trend in global SST, and vice versa) is identified throughout the forested regions of northwestern, western, central, and eastern Canada, with strongly correlated core regions in the Yukon and a boreal forest region extending from northern Alberta to Newfoundland. Areas possessing statistical significance at the 5% level are delineated by a dashed line. Southern Yukon and British Columbia

TABLE 1. Summary statistics of SVD analysis for Canadian summer (June–August) SSR data and preceding winter (December–February) and spring (March–May) global SST anomaly data and Canadian PDSI data, 1953–2007.

Mode	SCF (%)	r	NCF (%)
1	75.76	0.78	11.70
2	18.68	0.56	8.67
3	3.49	0.47	3.15

show weak positive or negative SSR correlation (low fire severity corresponding to strong warming trend in global SST, and vice versa); these values are not significant at the 5% level, however.

The heterogeneous correlation pattern for the second SVD mode (Fig. 6b) has significant negative correlations (high fire severity corresponding to strong cooling trend, and vice versa) in northern British Columbia, southern Yukon, and the Great Lakes–St. Lawrence lowlands and has positive correlations in central Yukon. This mode is weaker than the first mode. It is related to Pacific Ocean influences and identifies ENSO variability in the tropical Pacific and interdecadal variability in the central North Pacific. This mode shows that the positive phase of the PDO, along with the warm phase of ENSO (Figs. 5a,b), as identified by Zhang et al. (1997) and Deser and Blackmon (1995), leads to a high SSR over central Yukon and lower SSR over northern British Columbia, southern Yukon, and the Great Lakes–St. Lawrence lowlands. Skinner et al. (2006) found their third SST/SSR mode related to Pacific Ocean processes and showed strong positive correlation in western Canada and negative correlation in the lower Great Lakes region, with a pattern very similar to that of Fig. 6b.

b. Prediction skill

Figure 7 shows correlation, mean absolute error, and percent correct skill scores for the 1-year-out cross-validation forecast model. The geographical distribution of the correlation skill, averaged over 55 prediction models, is presented in Fig. 7a. A correlation skill of 0.30 or higher is locally statistically significant at the 5% level. Greater than 0.30 correlation skill is locally found over the Yukon and in an area extending from the northeastern Prairie Provinces through northern Ontario and central Quebec into Labrador and Newfoundland (with 5% significance level outlined with a thick dotted line). Correlation skill exceeds 0.6 over northern Saskatchewan and Manitoba, northern Ontario, and central Quebec. The statistical significance of spatially distributed data may be influenced by the number and interdependence of the data. Field significance (Livezey and Chen 1983), which represents the degree

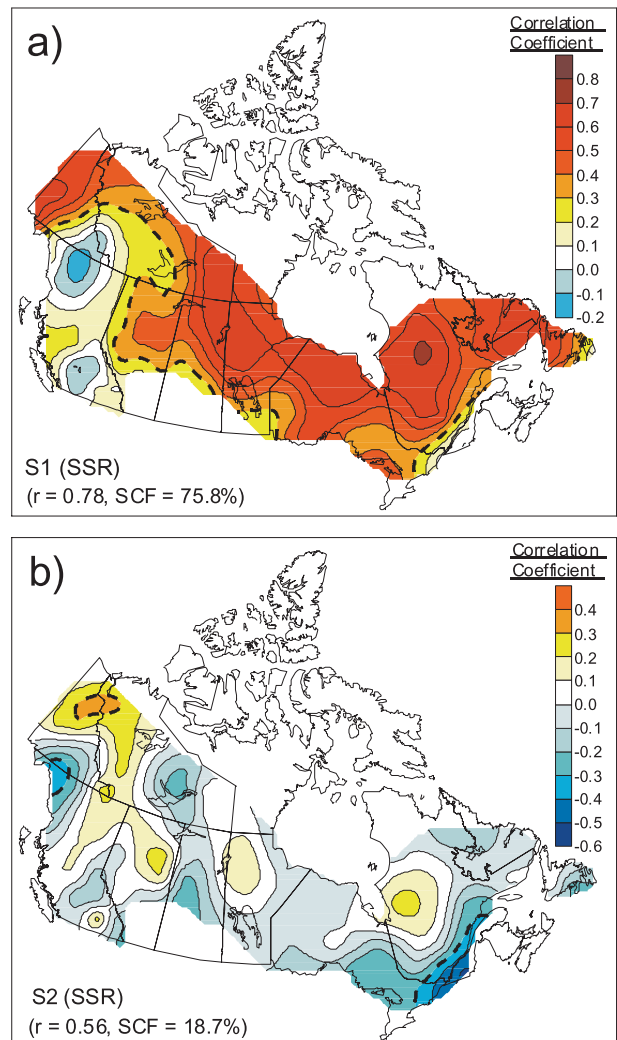


FIG. 6. (a) Heterogeneous correlation pattern of SSR for the first mode in the direct SVD expansion using global SSTs and Canadian PDSI. The temporal correlation coefficient between the corresponding expansion coefficients r and the SCF (%) is shown. (b) As in (a) but for the second heterogeneous correlation pattern of SSR. The contour interval is $r = 0.1$, and the 5% significance level is marked with a thick dotted line.

of statistical reliability, provides a measure of these effects. This statistic was evaluated by Monte Carlo simulation by randomly shuffling the forecast-to-observation year correspondence 1000 times and counting the number of times the mean of the actual explained variance statistics was exceeded by that of the random simulations. The values of 0.05 or less are considered significant. The results showed that the SSR forecast during the summer meets the field significance criteria at the 5% level. Figure 7b shows forecast error. The magnitude of the forecast error is given by the MAE. Areas of Canada exhibiting the highest correlation also correspond to the areas

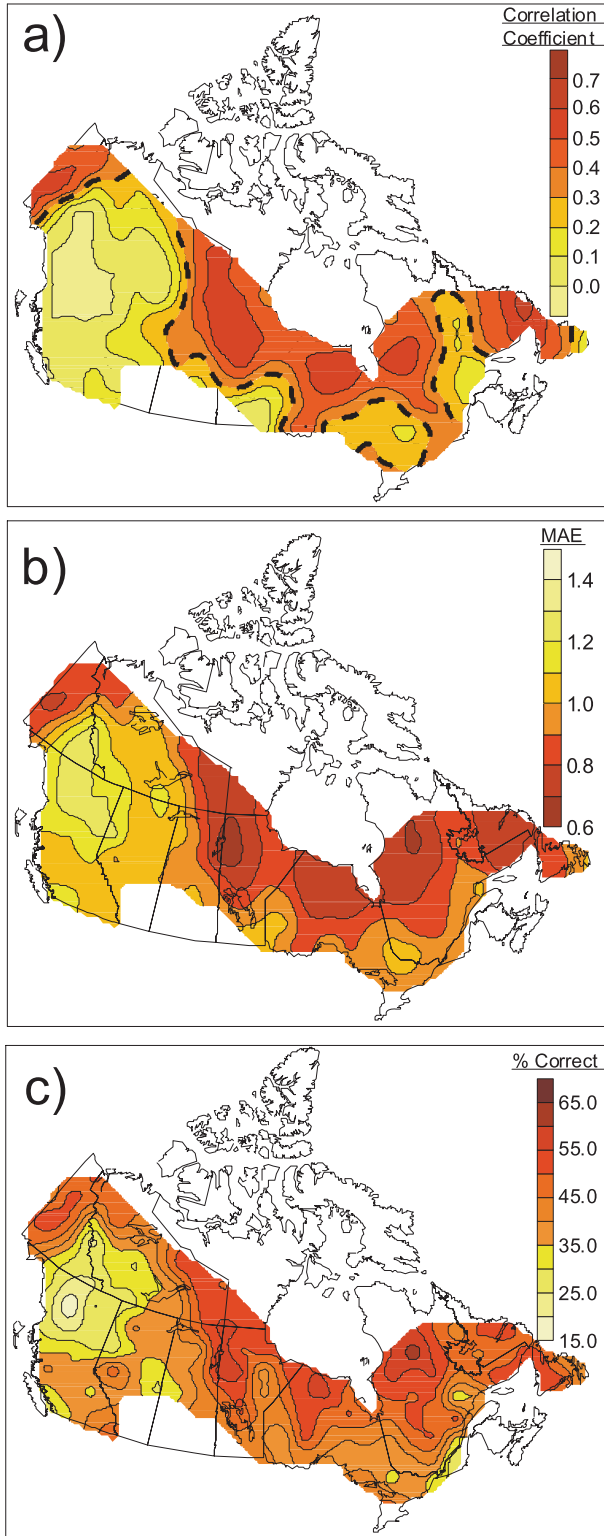


FIG. 7. (a) Prediction correlations (5% significance level is marked with a thick dotted line), (b) MAE, and (c) categorical forecast verification based on three equiprobable classes of summer SSR as predicted from winter and spring SST and PDSI.

TABLE 2. Number of occurrences within a given category expressed as percent and averaged over SSR grid locations for the 3-category 1-year-out forecast model. Most numbers of hits occur when both forecast and observed category are above normal or below normal.

		Forecast		
		Above	Normal	Below
Obs	Above	16.1%	7.7%	10.0%
	Normal	11.5%	12.4%	11.9%
	Below	6.9%	9.6%	13.7%

possessing the smallest MAE. The northeastern Prairie Provinces, northern Ontario, and central Quebec have MAE values of about 0.6. Categorical forecast verification (see section 3e) based on three equiprobable classes is shown in Fig. 7c. The forecast shows the highest skill, over 55% correct, in the Yukon and in an area stretching from the northeastern Prairie Provinces, northern Ontario, and central Quebec into Newfoundland. Forecast skill is the lowest in northern British Columbia. All three verification statistics reinforce each other and show skill in the same forested areas of Canada. Table 2 shows the contingency table for the 3-category forecast for the 1-year-out forecast model. The entries are number of occurrences in a given category expressed as percent of all occurrences, averaged over the SSR grid locations. Average number of hits is high when both forecast and observed are above normal (16.1%) or below normal (13.7%).

SSR forecasts were also verified on a 3-years-out cross-validation framework model. Average skills over the SSR grid points for the three verification statistics along with persistence skill are shown in Table 3. Correlation skills for the two cross-validation models are very similar to each other at approximately 0.33. While examining winter temperature forecast skill for Canada from the previous four seasons' global SST and Northern Hemisphere atmospheric circulation, Shabbar and Barnston (1996) found a similar national average correlation skill of about 0.36. Persistence forecast based on cross-validation framework yields an average correlation skill of 0.25. The overall percent correct skill is 42.2 for the 1-year-out model and 40.4 for the 3-years-out model, and the forecast based on persistence shows a lower skill of 39.1. The mean absolute error skill scores are very similar for the two cross-validation models at 0.95. The MAE based on persistence forecast is somewhat less skillful with a score of 1.5. These verification results show that there is little difference in the two cross-validation models, and that the persistence forecast is somewhat less skillful in all cases.

TABLE 3. Average correlation, percent correct, and mean absolute error skill scores over the SSR grid points for 1-year-out and 3-years-out cross-validation forecast models along with persistence forecast skill.

Score	1-yr-out cross validation	3-yr-out cross validation	Persistence
Correlation	0.33	0.31	0.25
Percent correct	42.2	40.4	39.1
MAE	0.94	0.96	1.5

5. Summary and discussion

The multivariate statistical technique of SVD is employed to explore prediction skill for summer forest fire severity in Canada. Results show reliable skill at a lead time of 3 months. Large-scale global oceanic processes and the PDSI moisture index over Canada have been identified as contributing factors to the skills. The spatial patterns of summer forest fire severity in Canada as represented by the SSR have been determined. The SSR is essentially a multivariate meteorological index combining the elements of air temperature, humidity, rainfall, and wind speed [over both short (hourly/daily) and long (weekly/monthly/seasonal) time scales] that influence the moisture content of forest fuels that determine whether a forest fire will start or spread. This SSR appears to possess potential predictability on a seasonal scale. The SVD linear prediction scheme forecasts patterns of the SSR. In addition, it generates diagnostics of the predictor patterns that lead to predictive skill and that may be used to explain statistical connections relating predictors and predictand. Nonlinear relationships between the predictors and predictand are not captured by the SVD technique.

In this study, a 3-month averaging period is used for the SSR. The evolving patterns of two consecutive 3-month periods lead to resulting patterns of the SSR. Although the overall correlation skill is around 0.33, regionally the skill can be much higher. For example, the SVD model explains 40%–50% of summer SSR variance over the northeastern Prairie Provinces. To a large extent, the global-climate trend in the SSTs and fluctuations associated with the ENSO phenomenon provide opportunities for prediction of summer forest fire severity in Canada. It is found that the lower boundary conditions represented by the global SST provide an important source of predictive skill. Experimentation shows that the leading mode of the SVD captures the long-term warming trend in the SST over the western Pacific and the Indian Ocean and also the influences of the multidecadal fluctuations related to the AMO in the North Atlantic. This, in combination with moisture conditions over Canada, affects summer fire severity.

The second mode is related to Pacific Ocean processes and the interrelationship between ENSO and the PDO and explains approximately 18% of the squared covariance. The lagged relationship between winter ENSO/PDO and the SSR is at least partially supported by the connection between the tropics and the North Pacific through the atmospheric bridge concept of Lau and Nath (1994) and by the Pacific–North American teleconnection pattern documented by Horel and Wallace (1981). Thus the warm phase of ENSO and positive phase of PDO, along with the moisture conditions (Figs. 5a,b)—most notably in the Mackenzie River basin (Fig. 3b)—are related to high SSR values. Assigning higher weights to the SST field increases cross-validation skill and emphasizes the effects of slow-varying boundary conditions. In addition, the relationship between the SST pattern and the SSR is more assured and the overfitting to accidental relationships in the short period of record is minimized.

These two leading coupled SVD modes of Canadian summer forest fire severity and global SST and Canadian drought index explain 95% of the squared covariance between the fields. Over the last four decades the western tropical SST of the Pacific and Indian Ocean has tended to warm while the high-latitude SST of the Pacific has tended to cool (Levitus et al. 2000). The trend mode coincides with drier conditions over much of Canada. Previous studies (Skinner et al. 1999, 2002; Podur et al. 2002; Stocks et al. 2002) have demonstrated the upward trend in TAB by wildland fires in Canada over the past three decades. Gillett et al. (2004) demonstrated that human-induced climatic change has significantly affected the area burned by forest fires in Canada. They showed this by first using output from a coupled climate model to show that greenhouse gas and sulfate aerosol emissions have made a detectable contribution to summer-season warming in regions of Canada where the area burned by forest fires has increased and then applying a statistical model to simulate temperature changes. Our results emphasize the importance of a warming trend in global SST in the determination of forest fires in Canada. This warming trend suggests that we may expect an increase in widespread fires in the boreal forests of Canada in coming decades.

One of the aims of this study was to develop a long-range fire-severity prediction scheme for Canada. The linear SVD technique provides a statistical method for this purpose. By projecting observed SSTs and drought fields onto the predictand SVD modes, it can be easily incorporated into an operational prediction scheme. Insofar as the global SSTs can be forecast with some accuracy, application of the statistical technique outlined in this paper can extend the lead time for SSR

forecasts, which may provide added guidance to forest-management officials.

In summary, SVD can skillfully predict summer forest fire severity with statistically significant skill at a lead of 3 months in Canada. The interdecadal trend, along with the interannual ENSO and interdecadal PDO fluctuations as well as the inclusion of winter and spring soil moisture estimates (including overwinter snowfall), identifies sources of statistical predictability for fire severity in Canada. In future, the availability of surface moisture analysis from the Land Data Assimilation System (LDAS; Rodell et al. 2004), which is based on more-sophisticated land surface models than those being used in the PDSI calculations, may improve the verification results reported here. At present, moisture estimates from these systems do not have the long record required for development of empirical prediction models.

Acknowledgments. The SSR index was computed from Meteorological Service of Canada hourly and daily weather data by Alan Cantin at the Canadian Forest Service Great Lakes Forestry Centre. Constructive and insightful comments from Kit Szeto, Hai Lin, and three anonymous reviewers are greatly appreciated.

APPENDIX

The Canadian Forest Fire Weather Index System

The Canadian forest fire danger rating system (CFFDRS) is a national system for rating the risk of forest fires in Canada and is fully described online (http://cwfis.cfs.nrcan.gc.ca/en_CA/background/summary/fdr). Forest fire danger rating systems produce qualitative and/or numeric indices of fire potential, which are used as guidelines in a wide variety of fire management activities. There are currently two subsystems being used extensively in Canada and internationally: the Canadian forest fire behavior prediction (FBP) system and the Canadian forest fire weather index system.

Calculation of the components of the FWI system is based on consecutive daily observations of temperature, relative humidity, wind speed, and 24-h rainfall. The FWI system is composed of six components that account for the effects of fuel moisture and wind on fire behavior (van Wagner 1987). The first three components are the fuel moisture codes: the fine fuel moisture code (FFMC), the Duff moisture code (DMC), and the drought code (DC). High values indicate dry fuels. The remaining three components are fire behavior indices. The FWI is a numeric rating of fire intensity. It represents the combination

of the initial spread index (ISI) and the buildup index (BUI). The FWI is suitable as a general index of fire danger throughout the forested areas of Canada. Equations for the computation of the five components are found in van Wagner and Pickett (1985).

The daily severity rating and its time-averaged value, the seasonal severity rating, are extensions of the FWI system. The DSR is a transformation of the daily FWI value, calculated as follows:

$$DSR = 0.0272(FWI)^{1.77}.$$

Higher FWI values are emphasized through the power relation. The DSR can be accumulated over time as the cumulative DSR, or it may be averaged over time as the SSR:

$$SSR = \frac{\sum_{i=1}^n DSR_i}{n},$$

where DSR_i is the DSR value for day i and n is the total number of days.

REFERENCES

- Alley, W. H., 1984: The Palmer drought severity index: Limitations and assumptions. *J. Climate Appl. Meteor.*, **23**, 1100–1109.
- Amiro, B. D., A. Cantin, M. D. Flannigan, and W. de Groot, 2009: Future emissions from Canadian boreal forest fires. *Can. J. For. Res.*, **39**, 383–395.
- Balshi, M. S., A. D. McGuire, P. Duffy, M. Flannigan, J. Walsh, and J. Melillo, 2008: Assessing the response of area burned to changing climate in western boreal North America using a multivariate adaptive regression splines (MARS) approach. *Global Change Biol.*, **15**, 578–600, doi:10.1111/j.1365-2486.2008.01679.x.
- Barnston, A. G., 1994: Linear statistical short-term climate predictive skill in the Northern Hemisphere. *J. Climate*, **7**, 1513–1564.
- Bonsal, B. R., and R. G. Lawford, 1999: Teleconnections between El Niño and La Niña events and summer extended dry spells on the Canadian prairies. *Int. J. Climatol.*, **19**, 1445–1458.
- Bretherton, C. S., C. Smith, and J. M. Wallace, 1992: An inter-comparison of methods for finding coupled patterns in climate data. *J. Climate*, **5**, 541–560.
- Collins, B. M., P. N. Omi, and P. L. Chapman, 2006: Regional relationships between climate and wildfire-burned area in the Interior West, USA. *Can. J. For. Res.*, **36**, 699–709, doi:10.1139/X05-264.
- Deser, C., and M. L. Blackmon, 1995: On the relationship between tropical and North Pacific sea surface temperature variations. *J. Climate*, **8**, 1677–1680.
- Enfield, D. B., A. M. Mestas-Núñez, and P. J. Trimble, 2001: The Atlantic multidecadal oscillation and its relation to rainfall and river flows in the continental U.S. *Geophys. Res. Lett.*, **28**, 2077–2080.

- Flannigan, M. D., and B. M. Wotton, 1989: A study of interpolation methods for forest fire danger rating in Canada. *Can. J. For. Res.*, **19**, 1059–1066.
- , and —, 2001: Climate, weather and area burned. *Forest Fires: Behavior and Ecological Effects*, E. A. Johnson and K. Miyanishi, Eds., Elsevier, 335–357.
- Gillett, N. P., A. J. Weaver, F. W. Zwiers, and M. D. Flannigan, 2004: Detecting the effect of climate change on Canadian forest fires. *Geophys. Res. Lett.*, **31**, L18211, doi:10.1029/2004GL020876.
- Girardin, M. P., and B. M. Wotton, 2009: Summer moisture and wildfire risks across Canada. *J. Appl. Meteor. Climatol.*, **48**, 517–533.
- Hoerling, M. P., and A. Kumar, 2003: The perfect ocean for drought. *Science*, **299**, 691–694.
- Horel, J. D., and J. M. Wallace, 1981: Planetary scale atmospheric phenomena associated with the Southern Oscillation. *Mon. Wea. Rev.*, **109**, 813–829.
- Keeton, W. S., P. W. Mote, and J. F. Franklin, 2007: Climate variability, climate change, and western wildfire with implications for the urban–wildland interface. *Living on the Edge: Economic, Institutional and Management Perspectives on Wildfire Hazard in the Urban Interface*, A. Troy and R. G. Kennedy, Eds., Advances in the Economics of Environmental Resources, Vol. 6, Elsevier, 225–253.
- Kitzberger, T., P. M. Brown, E. K. Heyerdahl, T. W. Swetnam, and T. T. Veblen, 2007: Contingent Pacific–Atlantic Ocean influence on multicentury wildfire synchrony over western North America. *Proc. Natl. Acad. Sci. USA*, **104**, 543–548.
- Lau, N.-C., and M. J. Nath, 1994: A modeling study of the relative roles of tropical and extratropical anomalies in the variability of the global atmosphere–ocean system. *J. Climate*, **7**, 1184–1207.
- , A. Leetma, and M. J. Nath, 2006: Attribution of atmospheric variations in the 1997–2003 period to SST anomalies in the Pacific and Indian Ocean basins. *J. Climate*, **19**, 3607–3628.
- Levitus, S., J. Antonov, T. Boyer, and C. Stephens, 2000: Warming of the World Ocean. *Science*, **287**, 2225–2229.
- Littell, J. S., D. McKenzie, D. L. Peterson, and A. L. Westerling, 2009: Climate and wildfire area burned in western U.S. eco-provinces, 1916–2003. *Ecol. Appl.*, **19**, 1003–1021.
- Livezey, R. E., and W. Y. Chen, 1983: Statistical field significance and its determination by Monte Carlo techniques. *Mon. Wea. Rev.*, **111**, 46–59.
- Mantua, N. J., S. R. Hare, Y. Zhang, J. M. Wallace, and R. C. Francis, 1997: A Pacific interdecadal climate oscillation with impacts on salmon production. *Bull. Amer. Meteor. Soc.*, **78**, 1069–1079.
- Mekis, E., and W. D. Hogg, 1999: Rehabilitation and analysis of Canadian daily precipitation time series. *Atmos.–Ocean*, **37**, 53–85.
- Meyn, A., S. Schmidlein, W. W. Taylor, M. P. Girardin, K. Thonicke, and W. Cramer, 2010: Spatial variation of trends in wildfire and summer drought in British Columbia, Canada, 1900–2000. *Int. J. Wildland Fire*, **19**, 272–283.
- Michaelsen, J., 1987: Cross-validation in statistical climate forecast models. *J. Climate Appl. Meteor.*, **26**, 1589–1600.
- Mitchener, L. J., and A. J. Parker, 2005: Climate, lightning, and wildfire in the national forests of the southeastern United States: 1989–1998. *Phys. Geogr.*, **26**, 147–162.
- Natural Resources Canada, cited 2009: The Canadian Wildland Fire Information System. [Available online at http://cwffis.cfs.nrcan.gc.ca/en_CA/background/summary/fdr/]
- Palmer, W. C., 1965: Meteorological drought. Weather Bureau Research Paper 45, 58 pp.
- Podur, J., D. L. Martell, and K. Knight, 2002: Statistical quality control analysis of forest fire activity in Canada. *Can. J. For. Res.*, **32**, 195–205.
- Rajagopalan, B., E. Cook, U. Lall, and B. K. Ray, 2000: Spatio-temporal variability of ENSO and SST teleconnections to summer drought over the United States during the twentieth century. *J. Climate*, **13**, 4244–4255.
- Rodell, M., and Coauthors, 2004: The Global Land Data Assimilation System. *Bull. Amer. Meteor. Soc.*, **85**, 381–394.
- Shabbar, A., and A. G. Barnston, 1996: Skill of seasonal climate forecasts in Canada using canonical correlation analysis. *Mon. Wea. Rev.*, **124**, 2370–2385.
- , and M. Khandekar, 1996: The impact of El Niño–Southern Oscillation on the temperature field over Canada. *Atmos.–Ocean*, **34**, 401–416.
- , and W. Skinner, 2004: Summer drought patterns and the relationship to global sea surface temperatures. *J. Climate*, **17**, 2866–2880.
- , and V. Kharin, 2007: An assessment of cross validation for estimating skill of empirical seasonal forecasts using a global coupled model simulation. *CLIVAR Exchanges*, No. 12, International CLIVAR Project Office, Southampton, United Kingdom, 10–12.
- , B. Bonsal, and M. Khandekar, 1997: Canadian precipitation patterns associated with the Southern Oscillation. *J. Climate*, **10**, 3016–3027.
- Skinner, W. R., B. J. Stocks, D. L. Martell, B. Bonsal, and A. Shabbar, 1999: The association between circulation anomalies in the mid-troposphere and area burned by wildland fire in Canada. *Theor. Appl. Climatol.*, **63**, 89–105.
- , J. B. Todd, M. D. Flannigan, D. L. Martell, B. J. Stocks, and B. M. Wotton, 2002: A 500 mb synoptic wildland fire climatology from large Canadian forest fires, 1959–1996. *Theor. Appl. Climatol.*, **71**, 157–169.
- , A. Shabbar, M. D. Flannigan, and K. Logan, 2006: Large forest fires in Canada and the relationship to global sea surface temperatures. *J. Geophys. Res.*, **111**, D14106, doi:10.1029/2005JD006738.
- Smith, T. M., and R. W. Reynolds, 2003: Extended reconstruction of global sea surface temperatures based on COADS data (1854–1997). *J. Climate*, **16**, 1495–1510.
- , and —, 2005: A global merged land–air–sea surface temperature reconstruction based on historical observations (1880–1997). *J. Climate*, **18**, 2021–2036.
- , —, T. C. Peterson, and J. Lawrimore, 2008: Improvements to NOAA’s historical merged land–ocean–surface temperature analysis (1880–2006). *J. Climate*, **21**, 2283–2296.
- Stocks, B. J., B. S. Lee, and D. S. Martell, 1996: Some potential carbon budget implications of fire management in the boreal forest. *Forest Ecosystems, Forest Management and the Global Carbon Cycle*, M. J. Apps and D. T. Price, Eds., NATO ASI Series, Series 1: Global Environmental Change, Vol. 40, Springer-Verlag, 89–96.
- , and Coauthors, 2002: Large forest fires in Canada, 1959–1997. *J. Geophys. Res.*, **107**, 8149, doi:10.1029/2001JD000484.
- Turetsky, M. R., B. D. Amiro, E. Bosch, and J. S. Bhatti, 2004: Historical burn area in western Canadian peatlands and its relationship to fire weather indices. *Global Biogeochem. Cycles*, **18**, GB4014, doi:10.1029/2004GB002222.
- van Wagner, C. E., 1987: Development and structure of the Canadian forest fire weather index system. Canadian Forest Service, Forestry Tech. Rep. 35, 37 pp.

- , and T. L. Pickett, 1985: Equations and FORTRAN programs for the Canadian forest fire weather index system. Canadian Forestry Service, Forestry Tech. Paper 33, 18 pp.
- Vincent, L. A., and D. W. Gullett, 1999: Canadian historical and homogeneous temperature datasets for climate change analyses. *Int. J. Climatol.*, **19**, 1375–1388.
- Wallace, J. M., C. Smith, and C. S. Bretherton, 1992: Singular value decomposition of wintertime sea surface temperature and 500-mb height anomalies. *J. Climate*, **5**, 561–576.
- Westerling, A. L., A. Gershunov, D. R. Cayan, and T. P. Barnett, 2002: Long lead statistical forecasts of area burned in western U.S. wildfires by ecosystem province. *Int. J. Wildland Fire*, **11**, 257–266.
- Willmott, C. J., and K. Matsuura, 2005: Advantages of the mean absolute error (MAE) over the root mean square error (RMSE) in assessing average model performance. *Climate Res.*, **30**, 79–82.
- Xiao, J., and Q. Zhuang, 2007: Drought effects on large fire activity in Canadian and Alaskan forests. *Environ. Res. Lett.*, **2**, 044003, doi:10.1088/1748-9326/2/4/044003.
- Zhang, Y., J. M. Wallace, and D. S. Batisti, 1997: ENSO-like interdecadal variability: 1900–93. *J. Climate*, **10**, 1004–1020.